ISIJ International, Vol. 49 (2009), No. 3, pp. 446–452

Characterization of Grain-boundary Precipitates after Hot-ductility Tests of Microalloyed Steels

Maurizo VEDANI,[1] David DELLASEGA[2] and Aldo MANNUCCII[3]

1) Politecnico di Milano, Dipartimento di Meccanica–Via G. La Masa 34, 20156 Milano, Italy. E-mail: maurizio.vedani@polimi.it
2) Politecnico di Milano, Dipartimento di Chimica, Materiali e Ingegneria Chimica–Piazza L. Da Vinci 32, 20133 Milano, Italy.
3) Tenaris Dalmine, IPRO/LP–Piazza Caduti 6 luglio 1944 1, 24044 Dalmine, Italy.

(*Received on September 4, 2008; accepted on December 8, 2008*)

The hot ductility of microalloyed steels was investigated by interrupted tensile tests at the temperatures of 850 and 950°C. Analyses of microstructural damage during plastic straining of the steels were performed using an experimental setup that allowed rapidly quenching the tensile specimens after straining to a predefined level. Microstructural investigations on the materials were carried out on longitudinally sectioned samples. Further analyses on crack surfaces were performed by fracturing the strained specimens in liquid nitrogen and by analyzing the surfaces formed by high-temperature decohesion through conventional and field emission SEM. It was demonstrated that AlN and Nb(C,N) precipitates, in isolated or combined form, affected the prior-austenite grain boundaries. Differences in hot cracking sensitivity among the steels was accounted for by modifications of the precipitate size and volume fraction.

KEY WORDS: microalloyed steels; hot ductility; intergranular fracture; grain-boundary precipitates.

1. Introduction

The loss in ductility experienced by steels during plastic deformation at temperatures generally ranging from 700 to 1 100°C is a widely studied subject in steel research. It has large practical implications especially for transverse cracking during continuous casting and for the development of cracks during forging of billets and plastic forming of wrought products.[1–3)]

Evaluation of steel sensitivity to hot cracking is usually carried out by drawing hot ductility curves, showing the reduction of area of specimens fractured in tension as a function of temperature. A typical hot-ductility curve distinctively shows an intermediate temperature region featuring a ductility trough where the embrittlement effect occurs with the highest evidence. It is well established that within this low-ductility region, fracture of the specimens always occurs by an intergranular mode and it can be caused by one or a combination of the following mechanisms. (i) Failure within a thin film of softer ferrite located at austenite grain boundaries. (ii) Formation of precipitate-free zones adjacent to austenite grain boundaries. (iii) Grain boundary sliding due to the limited dynamic recovery of austenite and due to build up of mismatch strains at triple joints of the grains (see for instance[4,5)]).

Grain boundary precipitates are detrimental to ductility because they stimulate void nucleation at ferrite films or during grain boundary sliding. They are also directly responsible for the formation of the precipitate-free zones adjacent to grain boundaries. Compositions and precipitation temperatures for many of the possible secondary phases in microalloyed steels have been stated in literature for many steel grades.[5–11)] From a literature survey it can be stated that AlN and (Nb, V)CN are generally considered as some of the most detrimental phases for hot ductility. However, when drawing information from published works, it is to consider that a great influence on precipitation sequence and on kinetics is exerted by the actual microstructural condition and the thermal history of the steel.[12–16)]

A relatively large number of papers available in literature refers to as cast steels tested by cooling at various rates from the melting temperature or by reheating the cast structure from room temperature.[1,2,6–9,12,13,17–20)] Under these conditions, the coarse grain structure and the segregation of alloying elements at boundaries strongly affects precipitation. On the contrary, less attention has been paid to hot ductility of wrought steels.[5,21)] Several investigations highlighted that for this condition, the effects promoted by the strain on precipitation mechanisms are of paramount importance. It is well known that straining at high temperature promotes dynamic precipitation mechanisms that accelerate the transformation kinetics and possibly lowers the precipitation temperatures of secondary phases.[14–16)] Wrought steels also feature a more homogeneous and finer grain structure that is expected to reduce the area fraction of secondary phases formed at grain boundaries.

Identification and characterization of grain boundary precipitates is therefore of great importance for the study of hot ductility of microalloyed steels. The experimental techniques generally adopted rely on analyses of the steel structure by transmission electron microscope (TEM) extraction replica[6,7,9,15,16,19)] or on fractographic studies of post

mortem specimens by a scanning electron microscope (SEM).[7,10,11,13,18,22] However, TEM replica can sample only small volumes of the material and they are rather time-consuming. On the contrary, morphological analyses by SEM can be much simpler but detailed analyses on submicron-size precipitates are often prevented by the oxidation of the broken samples and by the limited resolution of the microscope.

In the present paper, results on hot ductility of a series of microalloyed steels are presented. Analyses of possible microstructural damage during plastic straining of the steels were particularly performed using an experimental setup that allowed rapidly quenching tensile specimens right after straining to a predefined level. Further microstructural analyses on the surfaces of the hot cracks were carried out by fracturing the specimens in liquid nitrogen and by analyzing the surfaces formed by high-temperature decohesion through conventional and field emission SEM in combination with X-ray Energy Dispersive Spectrometer (EDS) microanalysis.

2. Materials Investigated

The investigations on hot ductility of several microalloyed steels was carried out starting from samples cut from commercially available products. The chemical composition of the steels investigated is given in **Table 1**. It can be inferred that different heats of the API X60 grade were considered to collect information on a range of steel compositions, of interest for steel pipe production.

3. Experimental Procedures

From previous experience it was established that the most critical temperatures for hot ductility of these steels lied within the range 850–950°C.[23] Details about the hot-ductility behaviour and on the resulting structure after hot straining was thus carried out at the temperature levels of 850°C and 950°C in ambient atmosphere, on samples in the as-supplied condition (samples cut from industrially quenched and tempered pipes).

The analyses described in the present paper consisted of interrupted tensile tests carried out up to a predefined strain level. Three levels of plastic strain corresponding to 10%, 17% and 30% at an initial strain rate of $2.8 \cdot 10^{-3}\,s^{-1}$ were considered. The highest value of strain roughly corresponded to the onset of necking for the steels investigated.

Analysis of possible microstructural damage that had occurred during plastic straining was then investigated by using an experimental setup that allowed rapidly quenching the specimens after straining so as to "freeze" the steel structure for further microstructural analyses. For this purpose, the fixturing device and load train depicted in **Fig. 1** was designed to pull in tension flat specimens having a gauge length of 50 mm and a rectangular section of $3 \times 10\,mm^2$ in a tubular resistance furnace. After having reached the expected strain level, the specimens could be rapidly separated from the fixtures and quenched in a water tank positioned below the furnace within a couple of seconds. The described experimental device was installed in a universal testing frame. Owing to the required rapid separation of the specimens from the load train for their quenching, the use of a high-temperature strain gauge was avoided. Therefore, the engineering strain was evaluated as the displacement of the testing frame divided by the full gauge length of the specimens.

Table 1. Chemical composition (mass%) of the materials investigated.

Code	C	Mn	Si	P	S	Al	N	Ti	Nb	V
A	0.1	1.07	0.27	0.015	0.001	0.023	0.0075	0.002	0.026	0.06
B	0.09	1.11	0.24	0.013	0.002	0.027	0.0053	0.001	0.022	0.042
C	0.11	1.08	0.24	0.014	0.002	0.028	0.0082	0.002	0.024	0.05
D	0.11	1.04	0.27	0.011	0.002	0.03	0.0080	0.003	0.023	0.05

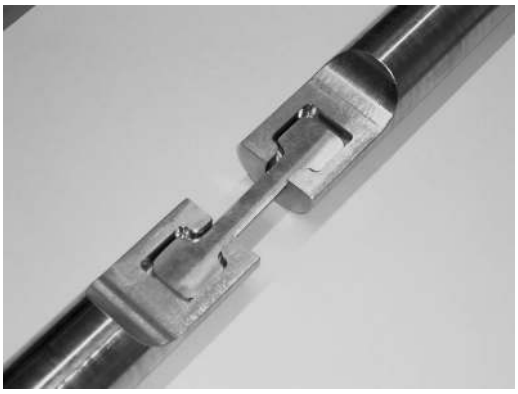

Fig. 1. View of a tensile specimen installed in the fixturing device.

The strained specimens were then subjected to different types of analyses. The grain structure and the defects formed at high temperature were first examined by optical and SEM analyses on metallographic samples cut longitudinally form the specimen gauge length. For this purpose, the samples were polished by standard metallographic techniques and chemically etched for 45 s in a solution of 8 g of $K_2S_2O_5$ in 100 mL of H_2O.

Fractographic analyses were carried out on the strained specimens by first fracturing them by an impact at the liquid nitrogen temperature. By this method, the low-temperature brittle fracture could be easily distinguished from the pre-existing damaged regions formed during high-temperature straining. In particular, fractographic observations allowed analysing the morphology of the clean, non oxidized faces of the hot cracks and the possible precipitates located on their surfaces, as depicted in **Fig. 2**. Qualitative information on chemistry of the precipitates lying on the surfaces of the hot cracks were collected by careful EDS microanalyses. Optimal microprobe resolution was obtained by selecting a relatively low accelerating voltage of the electron beam, so as to reduce the volume of material sampled, thus collecting more counts pertaining to secondary phases with a lower background signal coming from the surrounding steel matrix.

4. Results

Representative stress *vs.* strain plots of steel B are depicted in **Fig. 3**. The curves have been recorded during straining by 17 and 30%, at the temperatures of 850 and 950°C. From the stress *vs*. strain curves it can be stated that

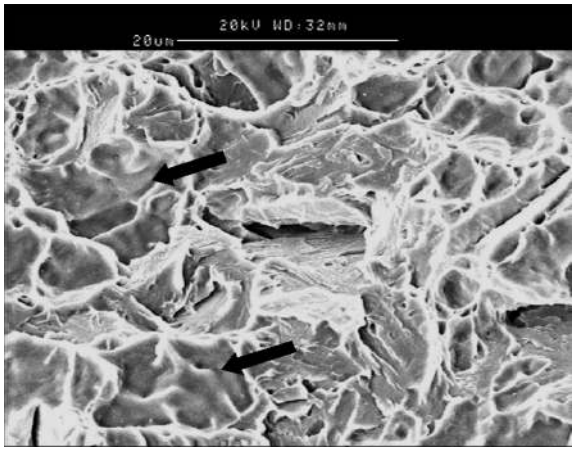

Fig. 2. Typical fracture surface aspect of a specimen pulled to 30% plastic strain at high temperature and fractured in liquid nitrogen after straining. The brittle cleavage surfaces generated by the low temperature fracture can be distinguished from the pre-existing high-temperature cracks (arrowed smooth surfaces).

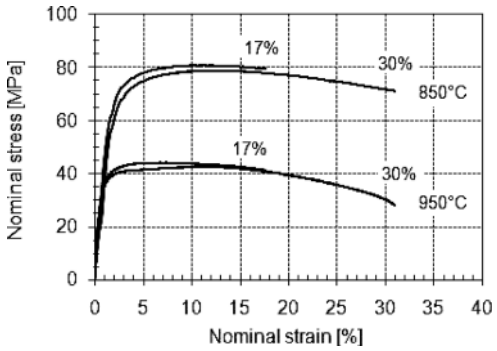

Fig. 3. Stress–strain curves recorded at 850 and at 950°C for steel B.

the plastic flow stress at 850°C is of the order of 80 MPa while it drops down to about 40 MPa for the test temperature of 950°C. For both temperatures the plastic flow develops homogeneously, without any evidence of sudden drop in the flow stress that could suggest the onset of dynamic recrystallization conditions or a rapid evolution of damage in the steel.

In **Figs. 4**(a) to 4(c) the microstructure of steel B after straining by 17% and 30% at 850 and 950°C is depicted. The optical micrographs were taken from longitudinally sectioned specimens at mid length of their gauge length (the loading direction is always horizontal in the following micrographs). The micrograph in Fig. 4(a) shows the duplex ferritic–martensitic structure of the steel that was generated as a consequence of the relatively low holding temperature (850°C) before straining and quenching. On the contrary, Figs. 4(b) and 4(c) highlight the fully martensitic structure of the steel obtained after hot straining at 950°C and water quenching, together with the prior-austenite grain boundaries. Intergranular cracks are clearly visible. These are preferentially oriented perpendicularly to the loading direction. A further example of the damage, taken at higher magnification by SEM is given for the same steel B in **Fig. 5**, showing in more details the intergranular character of the hot cracks.

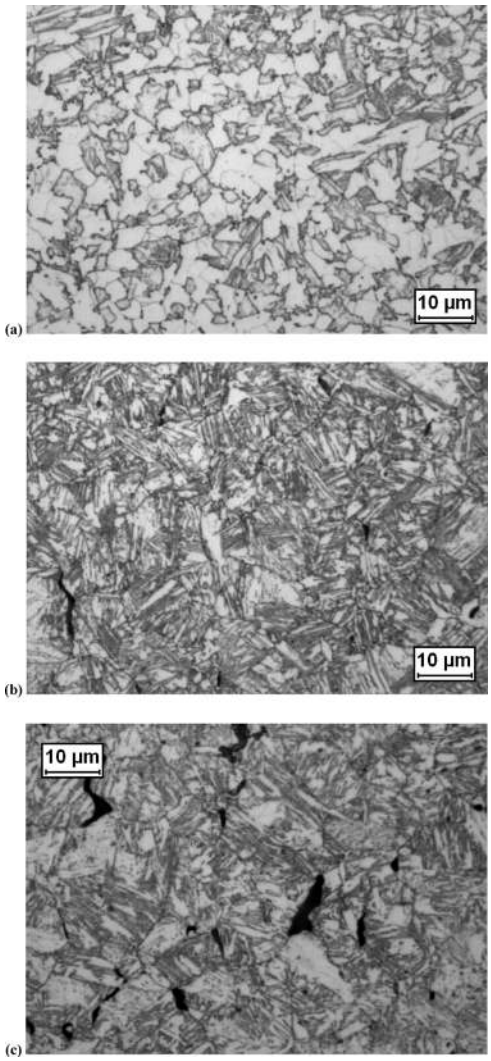

Fig. 4. Representative optical micrographs of steel B strained at 850°C by 17% (a) and at 950°C by 17% (b) and 30% (c).

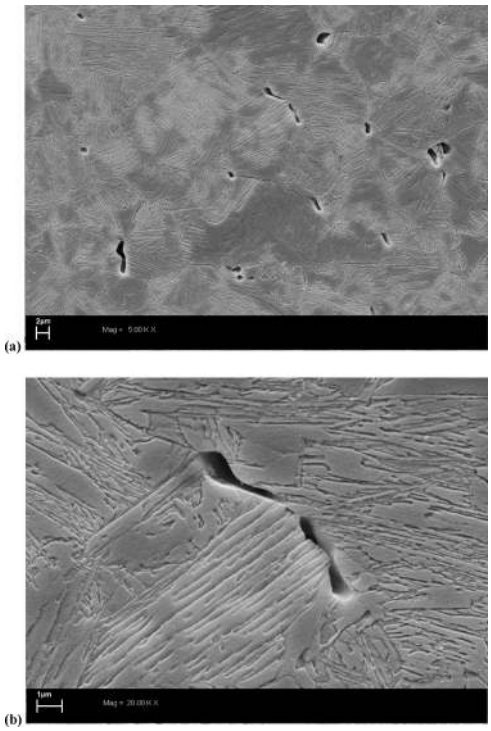

Fig. 5. SEM micrographs of steel B strained by 17% at 950°C.

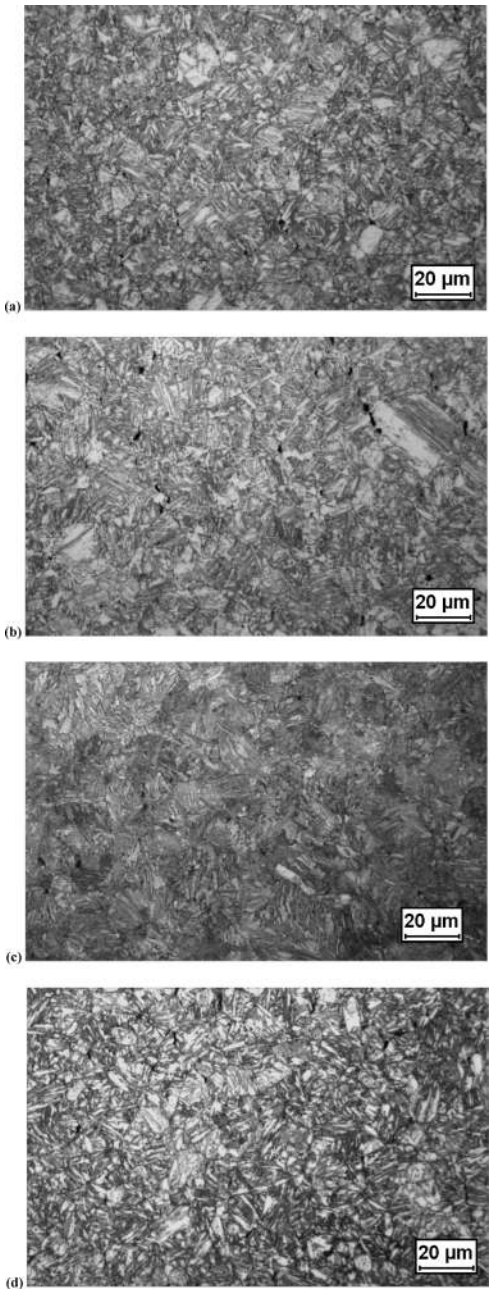

Fig. 6. Representative micrographs of the steels investigated, strained by 17% at 950°C. (a) Steel A, (b) steel B, (c) steel C, (d) steel D.

From the microstructural analyses performed by both optical and SEM microscopy, it was generally observed that, for the four steels here investigated, straining at 850°C to 10 and 17% produced only small cracks, hardly visible in the optical and SEM micrographs. Conversely, at the temperature level of 950°C, damage was clearly detectable especially in steels B and D already from 17% strain. **Figure 6** is a collection of representative optical micrographs of the four steels strained by 17% at 950°C, confirming the more extensive degree of damage found for steels B and D and the moderate cracking occurring in steels A and C. When increasing the strain level up to 30% at 950°C, cracking became much more evident in all of the steels investigated but it was still comparatively more developed in steels B and D.

To have an improved view of the intergranular crack surfaces, a set of samples pulled in tension at 950°C up to

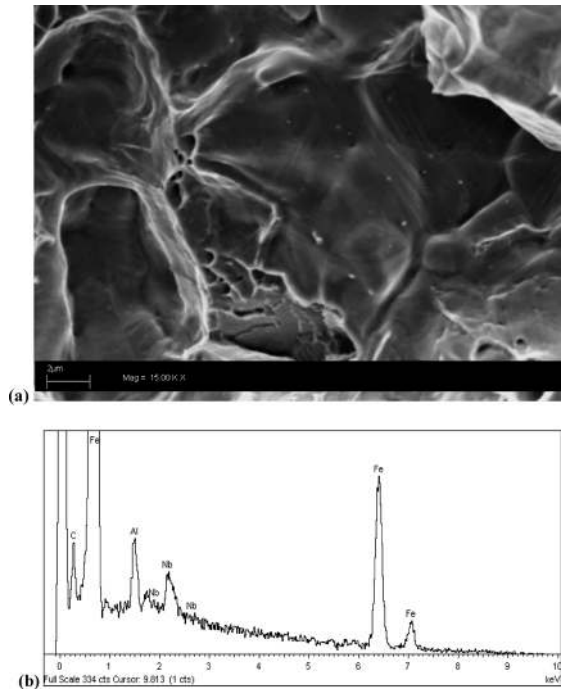

Fig. 7. Hot crack surface detected in steel A strained at 950°C (a) and typical EDS spectrum of the precipitates (b).

30% plastic strain was fractured into two halves after having been cooled into a liquid–nitrogen bath. It is to remark that analyses on the fractured samples were also performed on the materials strained at 850°C but the limited amount of damage detected prevented any statistically reliable analysis on precipitates to be performed. Morphological and microchemical analyses were then focussed on those regions appearing as flat surfaces, corresponding to the intergranular development of the hot cracks.

In **Fig. 7**(a) a typical SEM image is displayed together with an EDS spectrum taken in spot mode of the exposed precipitates (visible as the tiny white particles in the images, with a size of the order of 20–100 nm). The EDS spectrum clearly shows the presence of Nb and Al peaks together with the expected background signals of Fe, related to the matrix surrounding the analyzed precipitate. The spectrum depicted in the figure represents an example of a much larger population of particles analyzed by EDS microprobe. It was revealed that the main phases existing at grain boundaries are very often rich in Al and/or Nb. It is therefore supposed that both AlN and Nb(C, N) are the precipitates affecting grain boundaries. In agreement with literature, such particles could be found as isolated phases or in combined form (see for instance[6,7]).

Further FE-SEM analyses on the same samples were carried out in order to collect views at higher magnification of the fracture surface. It must be specified that by this equipment no substantial improvement in microprobe spatial resolution and detection sensitivity could be achieved whereas a significant improvement in morphological resolution on the tiny precipitates and on the fracture details was obtained. Therefore, FE-SEM analyses have been considered only on selected samples to acquire more detailed morphological images while SEM analyses were carried out routinely on the whole set of samples investigated.

The images reported in **Fig. 8** clearly support the hypoth-

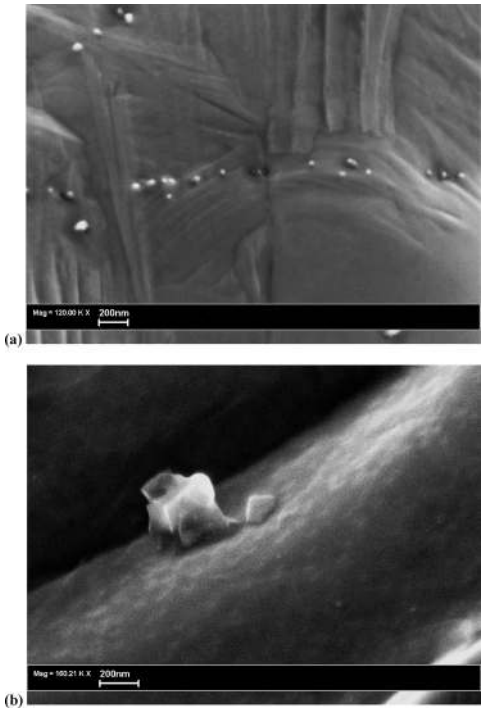

Fig. 8. FE-SEM images of the hot-crack surfaces showing the tiny precipitates originally decorating the austenite grain boundaries. (a) Steel A and (b) steel B, strained by 30% at 950°C.

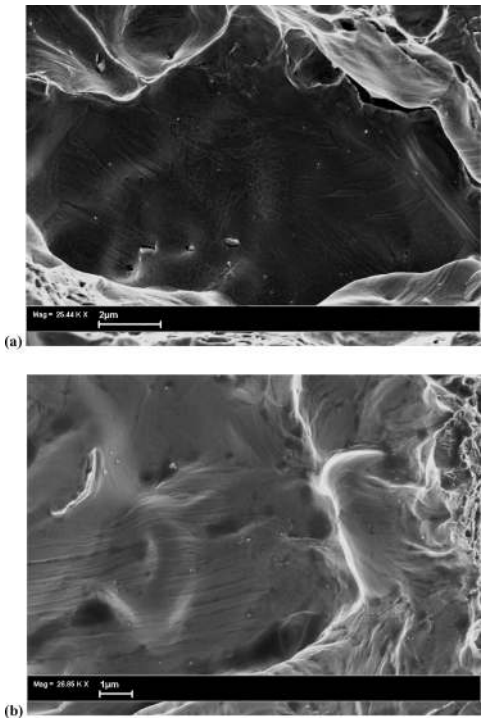

Fig. 9. FE-SEM images showing the morphological features of the hot-crack surfaces. (a) Steel B and (b) steel C, strained by 30% at 950°C.

esis that the above described AlN and Nb(C, N) precipitates were the only secondary phases that decorated the austenite grain boundaries of the investigated steels at high temperature. The absence of other, even smaller particles that could not have been resolved by the conventional SEM was therefore verified.

FE-SEM observations also allowed revealing with improved quality some shallow ridges and steps on the fractured grain boundaries (see Fig. 8(a) and **Fig. 9**). It is believed that these features could be the traces of the slip planes accommodating plastic deformation inside of the grains and/or groves related to relative movements of adjacent grains during sliding, suggesting that the main damage mechanism operating at 950°C in the steels investigated consists of grain boundary sliding.

5. Discussion

The experimental results collected about hot ductility of four heats of the API X60 steel grade allowed establishing some general trends that were not available in published literature. It was already mentioned that most of the published work on hot ductility refers to as cast billets processed by continuous casting. On the contrary, in the present investigation, wrought steels were investigated with an expected different microstructure. This derived from the thermo-mechanical cycles experienced during plastic forming, generally producing a smaller grain size, a more uniform alloying and trace-element distribution and a different second-phase population in terms of size, volume fraction, composition and particle location (*i.e.* intragranular *vs.* intergranular position).

Despite the expected more homogeneous and finer microstructure, it was revealed that significant intergranular cracking developed in some of the steels pulled in tension to 17% plastic strain at 950°C. Conversely, at the lowest temperature of 850°C, cracking was barely detectable in all the steels investigated. Analyses on surfaces of the hot cracks showed that the damage mechanism operating at 950°C in the steels mainly consisted of grain boundary sliding. This mechanism is generally different from what usually detected in cast steels of similar composition, for which grain-boundary sliding is of secondary importance and microvoiding from relatively coarse MnS inclusions or microalloying-element precipitates located at grain boundaries is the dominant fracture mode.[6,7,10,20,22] Of particular relevance for the present discussion is the work published by Zarandi and Yue[20] on transition between intergranular fracture based on microvoid coalescence and cracking promoted by grain-boundary sliding. These authors investigated in situ melted Nb-microalloyed steels subsequently strained to fracture at temperatures simulating the straightening stage in continuous casting strands. Their conclusions on the failure mechanisms demonstrated that the process of void formation occurred in combination with sliding at grain boundaries. It was further speculated that grain-boundary sliding is to be considered as a basic high-temperature deformation mechanism provided the relative deformation between neighbouring grains could be accommodated by plastic flow at grain interiors. Conversely, when plastic flow was hindered by the greater strength of microalloyed steels, boundary sliding would preferably be accommodated by cracking at boundaries, leading to increased steel brittleness. A combination of voiding and sliding at grain boundaries was also detected by Mohamed[5] investigating the hot ductility of V-containing steels.

For the wrought steels here investigated, it is therefore

supposed that that the presence of a fine grain-boundary precipitate distribution can more easily produce hot-cracking damage by stimulating crack nucleation during sliding rather than generating intergranular microvoiding, as is the rule for as cast steels. This concept was also highlighted in literature[4,5] and it was clearly confirmed by the present experimental analyses. Figure 9(a) can be taken as a clear example of this mechanism, showing small particles exposed on the fracture surfaces together with secondary voids nucleated at their boundaries.

By the analyses on the hot-crack surfaces it could be stated that a population of tiny precipitates having a size in the approximate range 20–100 nm decorated the grain boundaries of the hot-strained steels. High resolution FE-SEM observations also allowed excluding that further, even smaller, features at the grain boundaries were affecting the fracture behaviour of the steels. The EDS spectra collected during qualitative analyses of the precipitates showed that the particles affecting grain-boundary cohesion were rich in microalloying elements already recognized in other literature studies.[5–11] Typically AlN and Nb(C, N) were found in combined or isolated form, depending on specific particle analyzed. One of the microstructural parameters that was not possible to quantitatively assess in this study is the size distribution and amount (volume fraction) of the precipitates at austenite grain boundaries. Such information was barely considered also in other literature works owing to difficulties in quantitatively measuring the fine precipitates decorating grain boundaries on a reliable statistical basis. However, from a qualitative visual exam of the fracture surfaces produced at high temperature, it could be stated that the steels that revealed to be more prone to cracking during hot straining, generally showed a finer distribution of precipitates at grain boundaries. **Figure 10** is a comparison of representative hot-crack surfaces detected in steels A and B. The smaller average size of the precipitates found in steel B can be clearly recognized.

For the specific comparison among the four steels here investigated, it was thus supposed that, despite the similar chemical compositions of the heats, differences in thermomechanical history of the steels would have produced changes in the grain-boundary precipitate size that in turn generated marked effects on the hot-ductility behaviour. Hence, the different sensitivity of the steel samples here investigated was not set by the presence of a specific phase or by the amount of some alloying elements, but by the overall structure (at the submicrometer scale-size) of the grain boundaries.

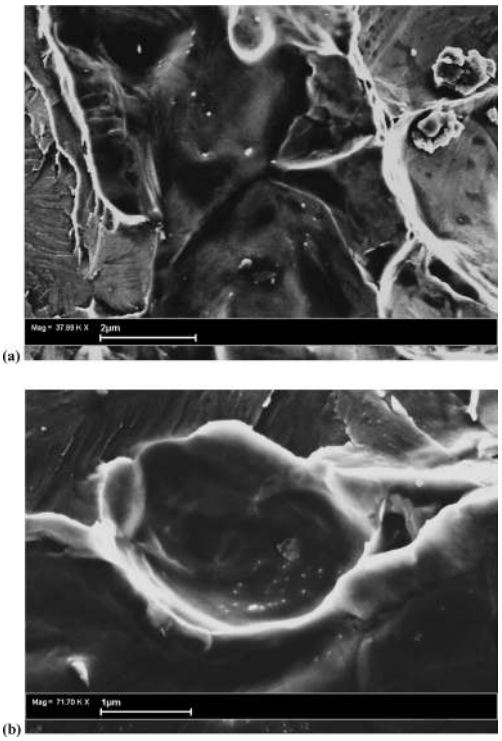

Fig. 10. FE-SEM images showing the average size of the particles exposed on the fracture surfaces. (a) Steel A and (b) steel B, strained by 30% at 950°C.

6. Conclusions

The present investigation was focussed on damage behaviour of several heats of the API X60-type steel, pulled in tension at 850 and 950°C to different strain levels. From experimental results it was observed that cracking during hot straining at the highest temperature level readily developed in some of the heats investigated.

The frame of results collected on hot-ductility of the four steel heats allowed establishing some general information on the damage mechanisms active in wrought steels. Differences were observed between the present materials and most of the cases presented in literature, mainly referred to as cast steels.

Analyses on the surfaces of the cracks formed during high-temperature straining showed that the damage mechanism operating at 950°C in the steels consisted of intergranular cracking promoted by grain boundary sliding and that the fine grain-boundary precipitates can deplete hot ductility by stimulating crack nucleation. It was stated that the particles affecting grain-boundary cohesion were typically AlN, or a combination of AlN with Nb(C, N).

It was further established that hot ductility of the steels was strongly affected by modifications of the distribution and size of precipitates, the development of cracks increasing with decreasing the size of the grain-boundary precipitates.

Finally, an experimental method based on interrupted hot-straining tests and analyses on the fracture facets of the hot cracks was proposed. The fractographic analyses carried out after specimen separation by brittle fracture in liquid nitrogen revealed to be a useful experimental method for a detailed identification and characterization of the grain boundary precipitates affecting fracture of the steels.

Acknowledgements

The authors would like to acknowledge the skilful experimental work carried out by Mr. P. Pellin, Dr. F. Moretto and Dr. D. Ripamonti. The permission to publish the results by Tenaris Dalmine is also greatly appreciated.

REFERENCES

1) B. Mintz: *ISIJ Int.*, **39** (1999), 833.
2) G. I. S. L. Cardoso, B. Mintz and S. Yue: *Ironmaking Steelmaking*, **22** (1995), 365.

3) B. Mintz, R. Abushosha and J. J. Jonas: *ISIJ Int.*, **32** (1992), 241.
4) B. Mintz, S. Yue and J. J. Jonas: *Int. Mater. Rev.*, **36** (1991), 187.
5) Z. Mohamed: *Mater. Sci. Eng.*, **A326** (2002), 255.
6) O. Comineli, R. Abushosha and B. Mintz: *Mater. Sci. Technol.*, **15** (1999), 1058.
7) R. Abushosha, O. Comineli and B. Mintz: *Mater. Sci. Technol.*, **15** (1999), 278.
8) R. Abushosha, R. Vipond and B. Mintz: *Mater. Sci. Technol.*, **7** (1991), 613.
9) K. Banks, A. Koursaris, F. Verdoorn and A. Tuling: *Mater. Sci. Technol.*, **17** (2001), 1596.
10) E. Lopez-Chipres, I. Mejia, C. Maldonado, A. Bedolla-Jacuinde and J. M. Cabrera: *Mater. Sci. Eng.*, **A460–461** (2007), 464.
11) F. Zarandi and S. Yue: *Metall. Mater. Trans. A*, **37A** (2006), 2316.
12) S. Akhalaghi and S. Yue: *ISIJ Int.*, **41** (2001), 1350.
13) F. Zarandi and S. Yue: *ISIJ Int.*, **44** (2004), 1705.
14) E. Valdes and C. M. Sellars: *Mater. Sci. Technol.*, **7** (1991), 622.
15) S. C. Hong, S. H. Lim, H. S. Hong, K. J. Lee, D. H. Shin and K. S. Lee: *Mater. Sci. Eng.*, **A355** (2003), 241.
16) E. V. Pereloma, B. R. Crawford and P. D. Hodgson: *Mater. Sci. Eng.*, **A299** (2001), 27.
17) H. Luo, L. P. Karjalainen, D. A. Porter, H. M. Liimatainen and Y. Zhang: *ISIJ Int.*, **42** (2002), 273.
18) J. Calvo, A. Rezaenian, J. M. Cabrera and S. Yue: *Engng. Fail. Anal.*, **14** (2007), 374.
19) C. Spradbery and B. Mintz: *Ironmaking Steelmaking*, **32** (2005), 319.
20) F. Zarandi and S. Yue: *Metall. Mater. Trans. A*, **35A** (2004), 3823.
21) H. Luo and P. Zhao: *Mater. Sci. Technol.*, **17** (2001), 1589.
22) E. Hurtado-Delgado and R. D. Morales: *Metall. Mater. Trans. B*, **32B** (2001), 919.
23) M. Vedani, D. Dellasega, M. Armengol, F. Zana, C. G. Tommasi and A. Mannucci: Proc. Int. Conf. on Microalloyed Steels, AIST, Pittsburg, (2007), 251.